FACTA UNIVERSITATIS
Series: **Electronics and Energetics** Vol. 37, Nº 4, December 2024, pp. 655 – 669
https://doi.org/10.2298/FUEE2404655M

Original scientific paper

DESIGN OF MULTIPLE-BEAM MICROSTRIP SMART ANTENNA FOR MASSIVE MIMO APPLICATIONS*

Manisha Mishra, Anindita Khan, Jibendu Sekhar Roy

School of Electronics Engineering, KIIT University, Bhubaneswar, Odisha, India

ORCID iDs:	Manisha Mishra	https://orcid.org/0000-0002-9635-4000
	Anindita Khan	https://orcid.org/0009-0005-8228-5568
	Jibendu Sekhar Roy	https://orcid.org/0000-0002-3571-2708

Abstract. *To improve the capacity of a radio communication system, MIMO (multiple input, multiple output) wireless technology is used, where multiple antennas are installed at both the transmission and reception ends. At the receiving end, by combining the received signals from all antennas, the fading effect can be reduced, which increases signal-to-noise ratio (SNR) and minimizes the error rate. Wireless networks in multi-user environments need massive MIMO (MMIMO) systems as multiple antenna networks. The MMIMO installs large antenna arrays in the base stations, using a large number of transceivers with other RF modules to produce a very narrow and targeted radiation beam with reduced interference. This paper describes the method of producing multiple targeted radiation beams using an MMIMO smart antenna system with a microstrip array. The sub-6 GHz band of 5 GHz is used for the design of multiple beam smart antennas. The adaptive signal processing algorithm least mean square (LMS) is used for the beamforming of microstrip smart antennas. The number of antenna elements in the smart antenna is varied from 30 to 45. In case of three beam formation, the achieved maximum side lobe level (SLL) is -13 dB and minimum null depth is -27 dB. In case of four beam formation, the achieved maximum side lobe level (SLL) is -12 dB and minimum null depth is -25 dB. There was no deviation of the generated beam directions from the target user directions.*

Key words: *Massive MIMO, microstrip antenna, multiple beam, signal processing, smart antenna*

1. INTRODUCTION AND RELATED RESEARCH WORK

The MIMO technology uses multiple antennas at both the transmitter end and receiver end to enhance the capacity and quality of the RF link using spatial diversity and spatial multiplexing [1-3]. The key concept of the massive MIMO system is to equip base stations with a large antenna array to serve many users simultaneously with the same time-frequency

Received February 27, 2024; revised April 28, 2024; accepted June 26, 2024
Corresponding author: Jibendu Sekhar Roy
School of Electronics Engineering, KIIT University, Bhubaneswar, Odisha, India
E-mail: drjsroy@kiit.ac.in

resource. In massive MIMO, advanced antenna technologies are used to produce radiation beams towards the predefined directions (Fig. 1), which reduces interference for other users by deploying larger antenna arrays [4-7]. One of the key building blocks of 5G new radio (5G NR) is MMIMO, which achieves multiple benefits to both network operators and end users [8, 9]. The key features of MMIMO are spatial diversity, spatial multiplexing, and beamforming. MMIMO systems use large antenna arrays at the base station for highly directive beam generation [10]. Beamforming technology in 5G MMIMO system can reduce noise. Several approaches are reported to generate highly directive beams in a MMIMO system [11-17]. In [11], for a massive MIMO system, the performances of both microstrip and dipole arrays are reported. In [12], a 12-port hybrid 5G MMIMO array is described for different LTE bands.

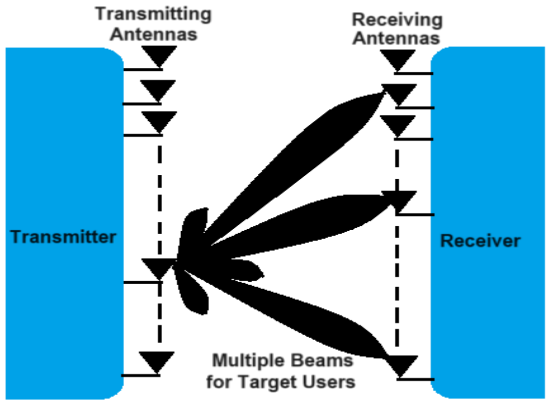

Fig. 1 Multiple radiation beams of a massive MIMO system

Different types of beamforming techniques in 5G MMIMO system are described [13, 14]. The report of [14] includes circular, planar, and conformal arrays. In [15], a full-rank channel matrix is used for a MMIMO antenna system in the presence of a small number of virtually positioned scatterers. In the review paper [16], the design and development of antenna techniques for future 5G MMIMO system are described. A metamaterial-loaded 64-element antenna system is designed in [17] for high efficiency and gain for millimeter-wave MMIMO systems. The smart antenna is one of the potential candidates for the generation of a beam towards the target user and a null towards the interferer for an MMIMO radio communication. The smart antenna enhances security, spectral efficiency, and power savings in a cellular network [18-24]. In [18], the design considerations and applications of smart antennas in wireless communication are described. Various signal processing algorithms are reported for the beamforming of smart antennas, whereas the implementation of the least mean square (LMS) algorithm and its variants [19, 20] is easier compared to other algorithms. Recently, deep learning methods have been used for the beamforming of smart antennas [21, 22]. The machine learning methods are also used for the bean formation of smart antennas [23]. For low energy consumption, an optimized thinned smart antenna design is reported in [24]. Microstrip antenna is one of the promising candidates for massive MIMO system. Smart antenna using microstrip antenna is reported in [25] for sector beamforming for 28GHz millimeterwave mobile communication. A hybrid beamforming method, using Chebyshev tapering, is presented in [26] for the application to massive MIMO systems. In [27], a beam design method is proposed where one beam is used to serve multiple transmissions, thus reducing the overhead of frequency beam adjustment. This method uses a fractional programming based algorithm to solve the problem. The improvement methods for the error rate in massive MIMO beamforming are reported in [28]. The beamforming design for a massive MIMO integrated sensing and communication system with imperfect channel state information was investigated in [29]. An orthogonal beamforming technique for multi-user massive MIMO system is proposed in [30].

The previous reports were devoted to single beam generation in a MMIMO system, which is not sufficient in a multi-user environment, and also in most of the papers, isotropic antenna elements are used for the smart antenna array. In this paper, to serve a large number of users in a 5G NR MMIMO system, a method of simultaneous multiple beam generation (one beam per user) from the same set of antenna elements, is proposed. A smart antenna of microstrip antennas is considered for the generation of targeted beams with multiple nulls towards the interferer. Because of thin and low profile nature of microstrip antennas, these are attractive for large array applications. The analysis of array factor for both an E-plane microstrip array and an H-plane microstrip array are presented. Multiple beams of microstrip smart antennas are formed using LMS algorithm in various user directions for particular null directions (interferer).

2. Theoretical Background of Microstrip Antenna

The multiple beams of a microstrip smart antenna are generated using the adaptive signal processing LMS algorithm. The basic form of a microstrip antenna is a radiating metallic patch fabricated on a dielectric substrate backed by a ground plane, as shown in Fig. 2(a), and it radiates only on the upper hemisphere [31, 32]. The antenna is excited by a co-axial SMA connector. Microstrip antennas are used in miniaturized microwave and millimeter-wave systems. In a linear array of microstrip antennas, the antennas are arranged in a line with uniform inter-element spacing, as shown in Fig. 2(b).

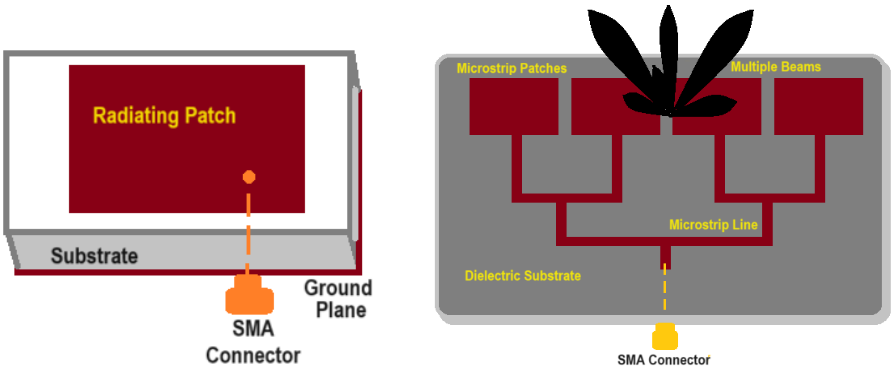

(a) (b)

Fig. 2 (a) Microstrip antenna (b) Multiple beams of a linear microstrip array

The resonance frequency at TM_{mn} mode for a microstrip antenna of dimension LxW can be calculated using the formula [32]

$$f_{rmn} = \left(c/2\sqrt{\varepsilon_e}\right)\sqrt{\left[\left(\frac{m\pi}{L}\right)^2 + \left(\frac{n\pi}{W}\right)^2\right]} \quad (1)$$

Where, 'c' is the free-space velocity of light and for a dielectric substrate of thickness 't', the effective dielectric constant (ε_r) is given by [32]

$$\varepsilon_e = (1/2)\left\{(\varepsilon_r + 1) + (\varepsilon_r - 1)\left(1 + \frac{12t}{W}\right)^{-1/2}\right\} \quad (2)$$

A microstrip array may be an E-plane array or an H-plane array, depending on the orientations of the patches and the mutual coupling between the antennas. The orientations of microstrip patches in E-plane and H-plane arrays are shown in Fig. 3.

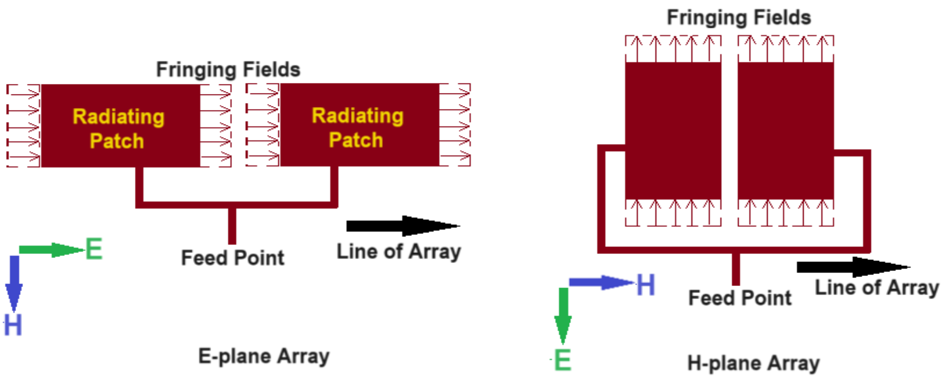

Fig. 3 E-plane and H-plane microstrip antenna arrays

The radiation pattern of a microstrip antenna can be calculated using Fig. 4. The radiating slots due to the fringing fields radiate on the upper hemisphere.

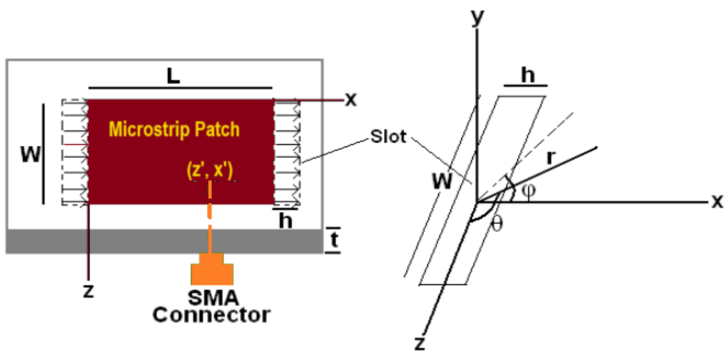

Fig. 4 Diagram to calculate radiation field of a microstrip antenna

The far field at a distance 'r' from the origin for a single slot is given by [31, 32].

$$E_{\varphi} = -j2V_0 W k_0 \left(e^{-jk_0 r} / 4\pi r \right) F(\theta, \varphi) E_{\theta} = 0 \tag{3}$$

V_0=tE_y is the voltage across the radiating slot and E_y is calculated considering a rectangular microstrip cavity, excited at fundamental TM_{10} mode.
Where

$$F(\theta, \emptyset) = \frac{\sin\left(\frac{k_0 h}{2}\sin\theta\, cos\emptyset\right)}{\frac{k_0 h}{2}\sin\theta\, cos\emptyset} \frac{\sin\left(\frac{k_0 W}{2} cos\theta\right)}{\frac{k_0 W}{2} cos\theta} sin\theta \tag{4}$$

For θ=π/2, F(φ), the E- plane (x-z plane) pattern can be determined from

$$F(\emptyset) = \frac{\sin\left(\frac{k_0 h}{2} cos\emptyset\right)}{\frac{k_0 h}{2} cos\emptyset} \cos\left(\frac{k_0 L}{2} cos\emptyset\right) \tag{5}$$

Slot width, h≈t/2, if t=1.6mm, and h=0.8mm

Similarly, for φ=π/2, F(θ), will represent H-plane(y-z plane),which is

$$F(\theta) = \frac{\sin\left(\frac{k_0 W}{2} cos\theta\right)}{\frac{k_0 W}{2} cos\theta} sin\theta \tag{6}$$

Depending on the orientation of microstrip patches in antenna array, E-plane or H-plane radiations are calculated.

A rectangular microstrip antenna is designed at 5GHz using CST Microwave Studio. The simulated S_{11} parameter and VSWR (voltage standing wave ratio) plots are presented in Fig. 5(a) and (b) respectively.

The antenna resonates at 5.016 GHz with return loss of 25.69 dB. The 2:1 VSWR bandwidth of the patch antenna is 200 MHz. The RT-Duroid substrate of dielectric constant 2.32, height 1.6 mm, and loss tangent [tan(δ)] 0.0005 is chosen for simulation.

A four-element microstrip array is simulated using CST Microwave Studio. The patch elements are connected by microstrip lines and excited by an SMA connector (Fig. 6).

The inter-element spacing in the array is 0.5λ. The S_{11} parameter and VSWR plot of the four-element patch array, for different feed line width (Wf in mm), are shown in Fig. 7 (a) and (b) respectively.

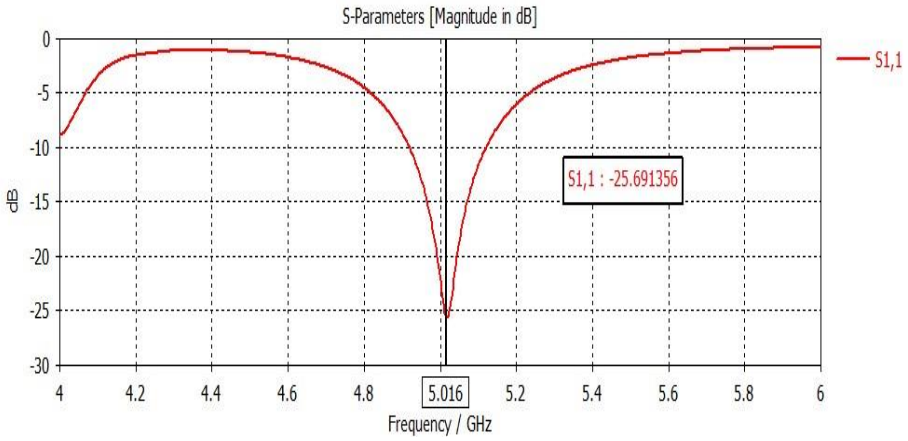

(a)

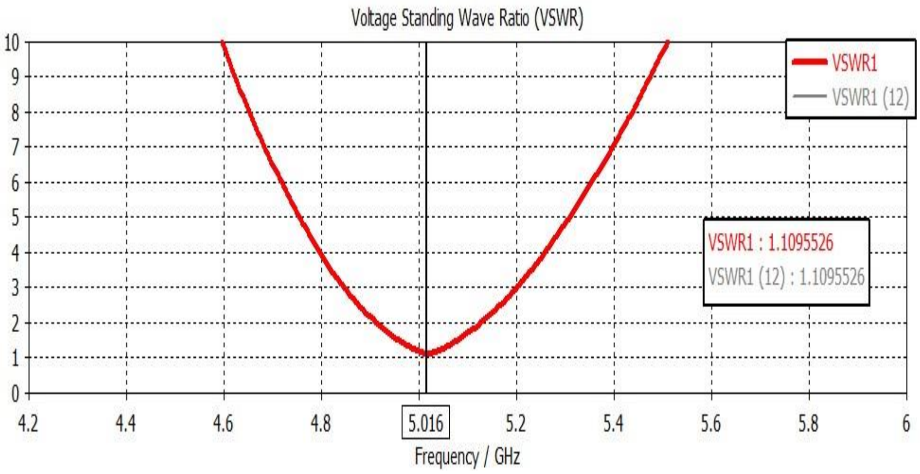

b)

Fig. 5 Simulated (a) S-parameter and (b) VSWR of the microstrip patch antenna

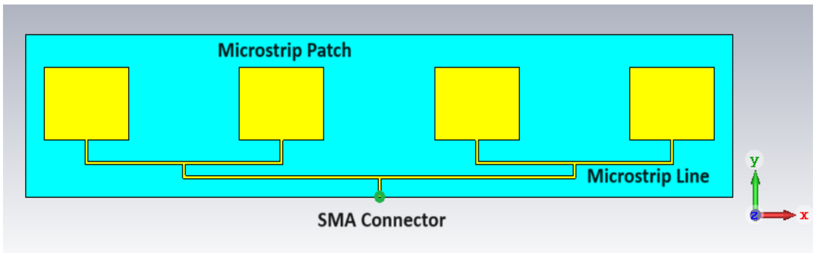

Fig. 6 Diagram of the simulated microstrip antenna array

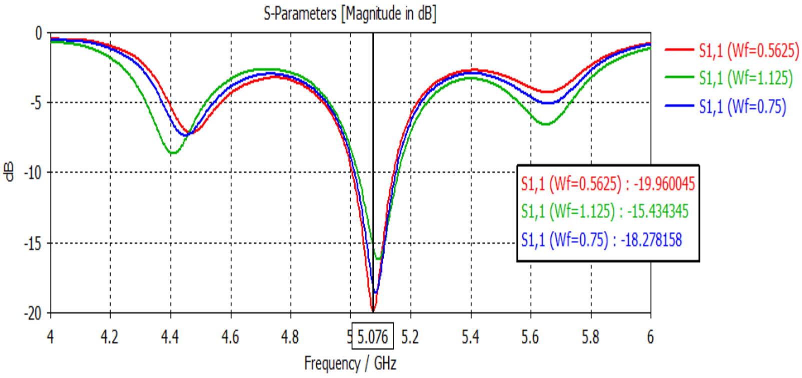

(a)

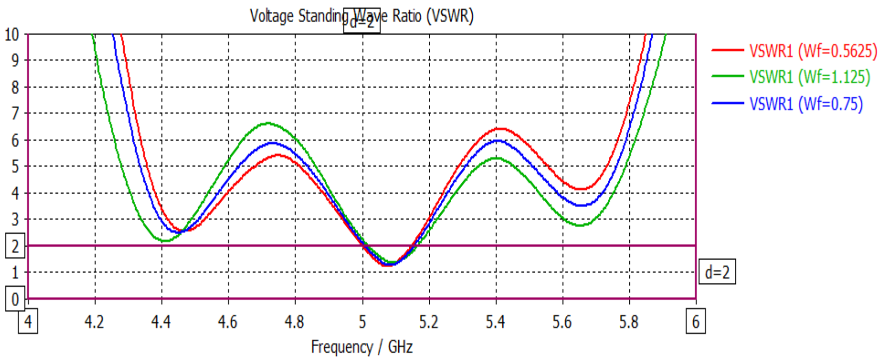

(b)

Fig. 7 (a) S_{11} parameter (b) VSWR

The radiation pattern of the microstrip array is shown in Fig. 8.

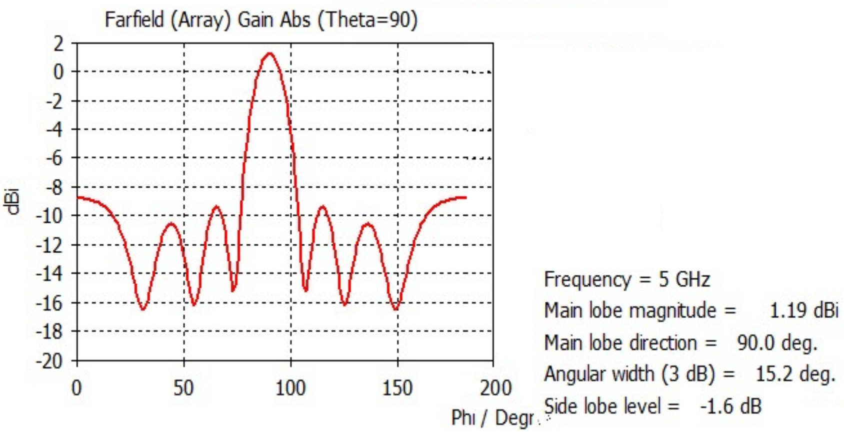

Fig. 8 Radiation pattern of four-element microstrip array

3. Multiple Beam Formation by Microstrip Smart Antenna

For the multiple beam formation, adaptive signal processing algorithm LMS is used. LMS is a stochastic gradient-based algorithm. The weights of the algorithm are updated in every iteration using the formula [33, 34]

$$w(n+1) = w(n) + \mu\, e^{*}(n)x(n) \tag{7}$$

The algorithm minimizes the error $e(n)$ between the array output $y(n) = w^{H}(n)x(n)$ and the desired signal $d(n)$ as

$$e(n) = d(n) - w^{H}(n)x(n) \tag{8}$$

Here, $w^{H}(n)$ is the Hermitian transpose or conjugate transpose of weight $w(n)$. The bound for the step-size parameter μ is given by

$$\mu < \frac{1}{2\, trace[R_{xx}]} \tag{9}$$

The R_{xx} is the correlation matrix. The LMS algorithm's main benefit is that it has a low level of computing complexity than other adaptive algorithms.

The LMS algorithm is used for the generation of beams towards the desired beam directions (BD) and for the generation of null directions (ND) towards the undesired interferers. The array factor (AF) for a linear microstrip array of N microstrip antennas and inter-element spacing of 'd', arranged in the E-plane, is

$$AF = \sum_{n=1}^{N} F(\emptyset)\; e^{j(n-1)(\frac{2\pi d}{\lambda}cos\theta + \alpha)} \tag{10}$$

Where, $F(\phi)$ is given by Eq. (5). The same expression of Eq. (10) is valid for H-plane microstrip array where $F(\phi)$ will be replaced by $F(\theta)$ of Eq. (6). The progressive phase shift of the array is 'α' at the wavelength 'λ'. The normalized array factor is

$$AF_{norm} = {|AF|}\Big/{|AF_{max}|} \tag{11}$$

The AF_{max} is the maximum value of AF.

The flow chart for the implementation of adaptive signal processing algorithm for multiple beam generation using microstrip smart antenna is shown in Fig. 9.

The input parameters are frequency, inter-element spacing in the antenna array, number of microstrip antennas, dielectric constant, and height of the microstrip substrate. Here, Eq. (1) and Eq. (2) are used to calculate the width (W) and length (L) of the patch antenna at the given frequency. The calculated length and width of the microstrip antenna at 5 GHz are 20.61 mm (L) and 18 mm (W). The values of the different parameters used in the simulation are presented in Table 1.

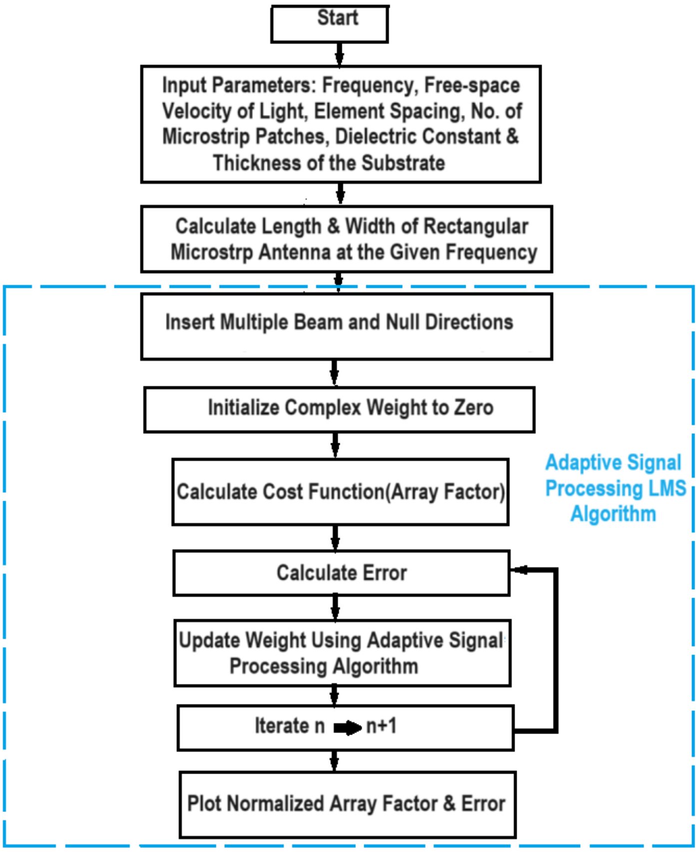

Fig. 9 Flow chart for multiple beam formation of microstrip smart antenna using LMS algorithm

Table 1 Input parameters

Input Parameters	Values
Frequency	5 GHz
Number of microstrip antennas in the array (N)	N=30, 35, 40, 45
Element spacing in the antenna array	0.5λ
Dielectric constant of the substrate (RT-Duroid)	2.32
Thickness of the dielectric substrate	1.6 mm
Channel	Additive white Gaussian noise (AWGN)
SNR	20 dB
No.of iteration	500

Eq. (10) with Eq. (6) is the cost function for AF calculation for an H-plane microstrip smart antenna. Here, using the LMS algorithm, three and four beams are generated for a microstrip smart antenna. Various values of the number of microstrip antennas in the array (N), beam directions (BD) and null directions (ND) are considered. The H-plane radiation patterns for three beams are shown in Figs. 10(a) -11(b). In Fig. 10(a) N= 30, BD=-45^0, 0^0, 30^0, and ND=-30^0,-15^0,10^0. In Fig. 10(b) N=35, BD= -60^0, 20^0, 45^0 and ND=-15^0, 10^0, 80^0. In Fig. 11(a) N=35, BD=-55^0, -20^0, 60^0 ND= -25^0,-15^0,10^0, and in Fig 11(b) N=30, BD= -35^0, 0^0, 60^0 ND= -60^0, -10^0, 15^0.

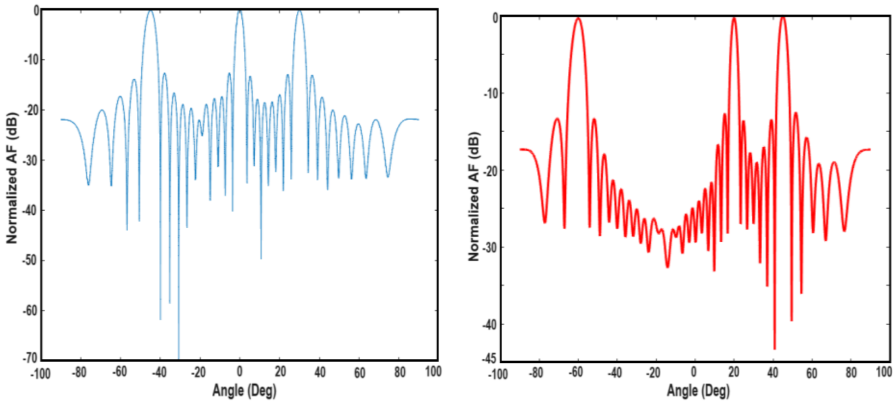

(a) (b)

Fig. 10 H-plane pattern for three beams for microstrip smart antenna (a) N=30, (b) N=35

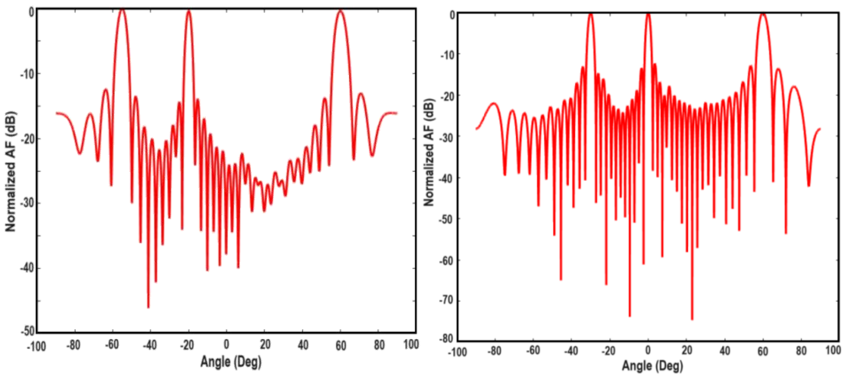

(a) (b)

Fig. 11 H-plane pattern for three beams for microstrip smart antenna (a) N=35, (b) N=30

In the above three beam formations, number of BDs are equal to number of NDs (interferer), but it is not mandatory, that is, while generating three beams, NDs may be 1 or 2 or 3 or 4.

The H-plane radiation patterns for four beams are shown in Figs. 12(a) -13(b). In Fig. 12(a) N=30, BD= -60^0, 0^0, 30^0, 50^0, and ND=-10^0, 10^0, 25^0. In Fig. 12(b) N=40, BD= -60^0, -25^0, 30^0, 60^0, and ND=-10^0, 10^0. In Fig. 13(a) N=40, BD=-55^0, -15^0, 10^0, 45^0, and ND= -10^0, 25^0, and in Fig 13(b) N=35, BD= -65^0, -15^0, 0^0, 55^0, and ND= -40^0, 25^0.

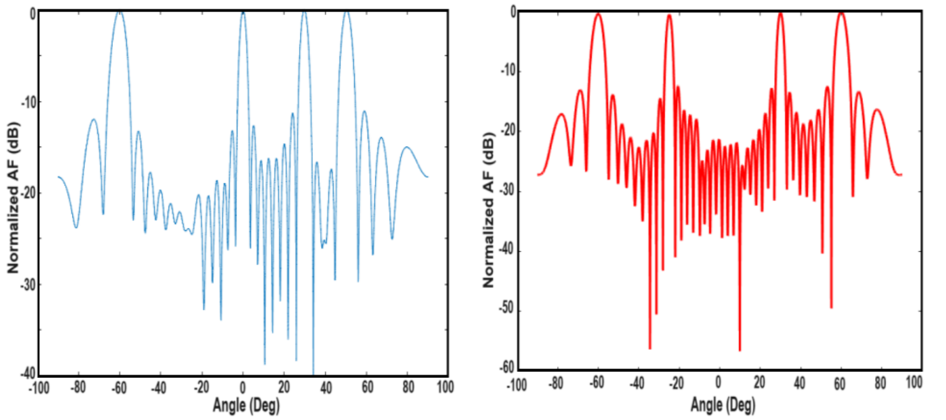

(a) (b)

Fig. 12 H-plane pattern for four beams for microstrip smart antenna (a) N=30, (b) N=40

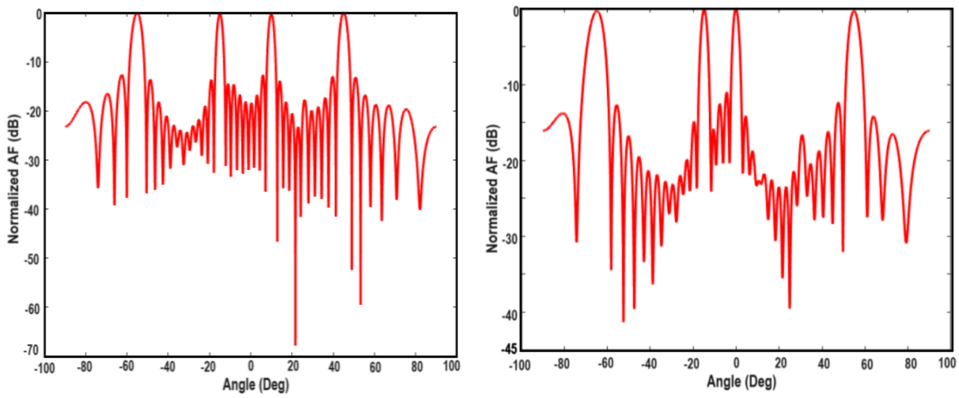

(a) (b)

Fig. 13 H-plane pattern for four beams for microstrip smart antenna (a) N=40, (b) N=35

The results are tabulated in Table 2. The HPBW, Null depth and SLL_{max} , obtained for generated multiple beams are included in the table. The multiple beams are generated on the both sides of the broadside direction of the array.

Null depth is one of the important parameters for MMIMO applications which signifies how much interference is occurred by the user signal. For multiple beam formation, for an E-plane microstrip smart antenna, Eq. (10) with Eq. (5) is the cost function for AF calculation. The same parameter values, mentioned in Table 1, are considered for the formation of three and four beams using a microstrip smart antenna. The E-plane radiation patterns for three and four beams are shown in Fig. 14 and Fig. 15 respectively. In Fig. 14(a) N=35, BD= 0^0, 20^0, 60^0, and ND=-60^0, -30^0, 10^0. In Fig. 14(b) N=40, BD=-55^0, -1^0, 15^0 and ND=10^0, 30^0. In Fig. 15(a) N=40, BD=-45^0, -10^0, 0^0, 30^0, and ND= -70^0, -40^0, 35^0, 45^0, and in Fig 15(b) N=45, BD= -20^0, -10^0, 35^0, 65^0, and ND=-45^0, -30^0, 15^0.

Table 2 Results for H-plane microstrip smart antenna

No. of beams	Parameters	Null depth	SLL_{max}
3 Beams	N= 30, BD=-45^0, 0^0, 30^0, ND=-30^0,-15^0,10^0	-70dB -37dB -48dB	-12 dB
3 Beams	N=35, BD= -60^0, 20^0, 45^0, ND=-15^0, 10^0, 80^0	-32dB -31dB -27dB	-13 dB
3 Beams	N=35, BD=-55^0, -20^0, 60^0, ND= -25^0,-15^0,10^0	-34dB -32dB -30dB	-12.5 dB
3 Beams	N=30, BD= -35^0, 0^0, 60^0 ND= -60^0, -10^0, 15^0.	-46dB -73dB -40dB	-12 dB
4 Beams	N=30, BD=-60^0,0^0,30^0,50^0 ND=-10^0,10^0,25^0	-25dB -38dB -37dB	-11.5 dB
4 Beams	N=40, BD= -60^0, -25^0, 30^0, 60^0 ND= -10^0, 10^0	-35dB -57dB	-12 dB
4 Beams	N=40, BD=-55^0, -15^0, 10^0, 45^0, ND= -10^0, 25^0	-32dB -40dB	-11 dB
4 Beams	N=35, BD= -65^0, -15^0, 0^0, 55^0, ND= -40^0, 25^0	-33dB -40dB	-12 dB

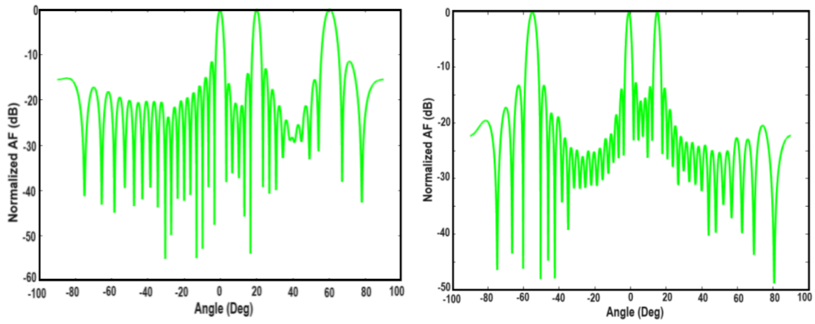

(a) (b)

Fig. 14 E-plane pattern for four beams for microstrip smart antenna (a) N=35, (b) N=40

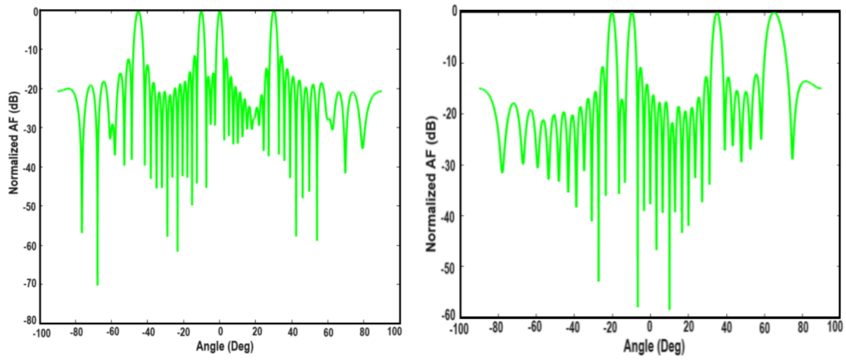

(a) (b)

Fig. 15 E-plane pattern for four beams for microstrip smart antenna (a) N=40, (b) N=45

The different parameters, obtained for E-plane microstrip smart antenna are tabulated in Table 3.

Table 3 Results for E-plane microstrip smart antenna

No. of beams	Parameters	Null depth	SLL_{max}
3 Beams	N=35, BD=0^0, 20^0, 60^0 , ND=-60^0, -30^0, 10^0	-45dB -55dB -40dB	-12 dB
3 Beams	N=40, BD=-55^0, -1^0, 15^0 , ND=10^0, 30^0	-27dB -32dB	-13 dB
4 Beams	N=40, BD=-45^0,-10^0,0^0, 30^0, ND=-70^0,-40^0, 35^0, 45^0	-70dB -42dB -43dB -48dB	-11.5dB
4 Beams	N=45, BD=-20^0, -10^0, 35^0, 65^0, and ND=-45^0, -30^0, 15^0	-33dB -52dB -42dB	-11 dB

The graph for square errors both for an H-plane array and an E-plane are array are shown in Fig. 16(a) and Fig. 16(b). Here, in both the cases, N=35, BD=-60^0, -25^0, 25^0, 40^0, and ND=10^0, -10^0.

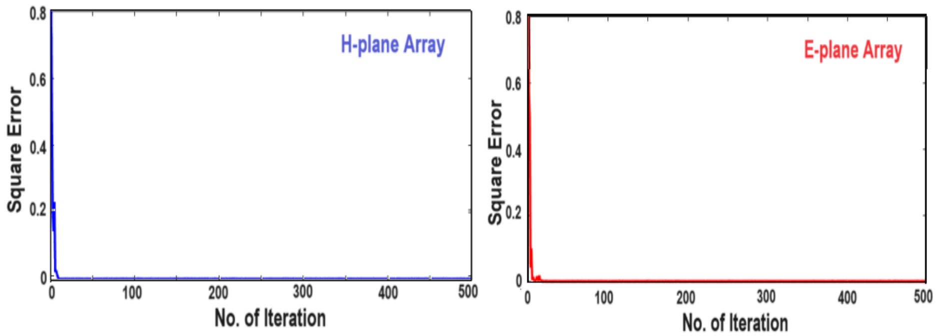

(a) (b)

Fig. 16 Error graphs for microstrip smart antenna

Number of iteration used in simulation is 500.

4. Conclusion

In a MMIMO system, where microstrip antennas are closely spaced in a large antenna array, an H-plane array may be useful to avoid the mutual coupling effect, because the H-plane coupling effect is less than the E-plane coupling. In order to have a basic idea, a microstrip antenna and a four-element microstrip antenna array are simulated using CST software. Their results are also presented. But this software doesn't consider signal processing algorithm, and hence, beam control regarding main beam generation in the desired direction and null generation towards the interferer is not possible. The results presented here are the best results obtained after a number of simulations in each and every case. The method presented here can generate multiple beams both when the target users are close and when the target users are far from each other. In MIMO system transmitting antenna radiates multiple beams towards the target receiving antenna and the antennas are diversity antennas not an array but in a MMIMO systems, the antenna system is an antenna array and radiation beam is sent single targeted beam per user basis. Therefore, the investigations, presented in this paper, are useful for MMIMO communication. Also, the proposed multiple beamforming method is well suited for millimeter wave massive MIMO.

REFERENCES

[1] A. J. Paulraj, D. A. Gore, R. U. Nabar and H Bolcskei, "An Overview of MIMO Communications-a Key to Gigabit Wireless", In Proceedings of the IEEE, 2024, vol. 92, no. 2, 198–218.

[2] M. R. Amin and S. D. Trapasiya, "Space Time Coding Scheme for MIMO System-literature Survey", *Procedia Eng.* vol. 38, pp. 3509–3517, 2012.

[3] S. Yang and L. Hanzo, "Fifty Years of MIMO Detection: The Road to Large-scale MIMOs", *IEEE Communication Survey Tutor,* vol. 17, pp. 1941–1988, 2015.

[4] E. G. Larsson, O. Edfors, F. Tufvesson and T.L. Marzetta, "Massive MIMO for Next Generation Wireless Systems", *IEEE Communication Magazine*, vol. 52, no. 2, pp. 186–195, 2014.

[5] P. Ranjan, S. Yadav and A. Bage, "Dual Band MIMO Antenna for LTE, 4G and Sub–6 GHz 5G Applications", *FACTA Universitatis Series Energetics and Electronics*, vol. 36, no. 1, pp. 43–51, 2023.

[6] Y. Su, H. Gao and S. Zhang, "Secure Massive MIMO System With Two-Way Relay Cooperative Transmission in 6G networks", *EURASIP Journal on Wireless Communications and Networking*, vol. 2023, no. 73, pp. 1–22, 2023.

[7] A. Khan and J. S. Roy, "Thinned Smart Antenna of a Semi-Circular Dipole Array for Massive MIMO Systems", *Advanced Electromagnetics*, vol. 12, no. 4, pp. 17–25, Dec. 2023.

[8] F. Wen, H. Wymeersch, B. Peng, W. P. Tay, H. C. So and D. Yang, "A Survey on 5G Massive MIMO Localization", *Digit. Signal Process.* vol. 94, pp. 21–28, 2019.

[9] M. Belgiovine, K. Sankhe, C. Bocanegra, D. Roy and K. R. Chowdhury, "Deep Learning at the Edge for Channel Estimation in Beyond-5G Massive MIMO", *IEEE Wireless Communication.* vol. 28, pp. 19–25, 2021.

[10] J. Hoydis, S. Brink and M. Debbah, "Massive MIMO in the UL/DL of Cellular Networks: How Many Antennas do We Need?", *IEEE J Selected Areas Communication*, vol. 31, no. 2, pp. 160–171, 2023.

[11] C.-M. Chen, V. Volski, L.V.D. Perre, G.A.E. Vandenbosch and S. Pollin, "Finite Large Antenna Arrays for Massive MIMO: characterization and system impact", *IEEE Trans. Antennas Propag*, vol. 65, no. 12, pp. 6712–6720, 2017.

[12] Y. Li, C.-Y.-D. Sim, Y. Luo and G. Yang, "12-port 5G Massive MIMO Antenna Array in Sub-6GHz Mobile Handset for LTE Bands 42/43/46 Applications", *IEEE Access*, vol. 6, pp. 344–354, 2017.

[13] E. Ali, M. Ismail, R. Nordin and N. F. Abdulah, "Beamforming Techniques for Massive MIMO Systems in 5G: Overview, Classification, and Trends for Future Research", *Frontiers of Information Technology & Electronic Engineering*, vol. 18, no. 6, pp. 753–772, 2017.

[14] A. M. Saleh, M. M. Elmesalawy, K. R. Mahmoud and I. I. Ibrahim, "Impact of Different Finite MIMO Array Geometries on System Throughput with Considering Mutual Coupling and Edge Effect between Array Elements", *Ain Shams Engg. Journal*, vol. 12, no.3, pp. 2823–2838, 2021.

[15] K. Honda, "Over-the-air Testing of a Massive MIMO Antenna with a Full-rank Channel Matrix", *Sensors*, vol. 22, no. 3, pp. 1–12, Feb. 2022.

[16] S. K. Ibrahim, M. J. Singh, S. S. Al-Bawri, H. H. Ibrahim, M. T. Islam, M. S. Islam, A. Alzamil and W. M. Abdulkawi, "Design, Challenges and Developments for 5G Massive MIMO Antenna Systems at sub 6-GHz Band: A Review", *Nanomaterials*, vol. 13, no. 3, pp. 1–40, Jan 2023.

[17] A. A. Musaed, S. S. Al-Bawri, W. M. Abdulkawi, K. Aljaloud, Z.Yusoff and M. T. Islam, "High Isolation 16-port Massive MIMO Antenna Based Negative Index Metamaterial for 5G mm-wave Applications", *Scientific Reports*, vol. 14, no. 290, pp. 1–11, Jan. 2024.

[18] M. Chryssomallis, "Smart Antennas", *IEEE Antennas & Propagation Magazine*, vol. 42, no. 3, pp. 129–136, June 2000.

[19] Veerendra and M. Bakhar, "A Novel LMS Beamformer for Adaptive Antenna Array", *Procedia Computer Science*, vol. 115, pp. 94–100, 2017.

[20] B. Samantaray, K. K. Das and J. S. Roy, "Performance of Smart Antenna in Cellular Network Using Variable Step-Size Algorithms", *International Journal of Microwave and Optical Technology (IJMOT)*, vol. 15, no. 2, pp. 179–186, March 2020.

[21] I. L. Bendjillali, M. S. Bendelhoum, A. A. Tadjeddine and M. Kamline, "Deep Learning-Powered Beamforming for 5G Massive MIMO Systems", *Journal of Telecommunication and Information Technology*, vol. 4, no. 4, pp. 38–45, Oct 2023.

[22] B. Samantaray, K. K. Das and J. S. Roy, "Comparison of the Performance of Artificial Neural Network with Variable Step-size Adaptive Algorithms for the Beamforming of Smart Antenna for Cellular Networks", *FACTA Universitatis Series: Electronics and Energetics Journal*, vol. 37, no. 2, pp. 277–287, 2024.

[23] B. Samantaray, K. K. Das and J. S. Roy, "Designing Smart Antennas Using Machine Learning Algorithms", *Journal of Telecommunication and Information Technology*, vol. 2023, no. 4, pp. 46–52, Oct 2023.

[24] A. Khan and J. S. Roy, "Design of Thinned Smart Antenna of Semi-circular Dipole Array for 5G Massive MIMO System" *FACTA Universitatis Series: Electronics and Energetics Journal*, vol. 37, no. 3, pp. 409–422, 2024.

[25] A. Halder, A. Senapati, and J. S. Roy, "Smart Antenna of Microstrip Array for Sector Beamforming for 28GHz Millimeterwave Mobile Communication", *International Journal of Microwave and Optical Technology (IJMOT)*, vol. 13, no. 3, pp. 203–208, May 2018.

[26] A. Jumaah, and A. Qaseem, "Hybrid Beamforming for Massive MIMO In 5G Wireless Networks", *4th Al-Noor International Conference for Science and Technology*, Istanbul, Turkey, 17–18 Aug. 2022, pp. 1–11, 2022.

[27] Y. Hu, K. Kang, S. Majhi, and H. Quin, "Downlink beamforming design for mobile users in massive MIMO system", *Digital Signal Processing*, Elsevier, vol. 30, article ID. 103716, Oct. 2022.

[28] A. B. Moniem, and M. M. Abdellatif, "Massive MIMO Beamforming Analysis for 5g Systems", Proceedings of 10th Intl. Conference on Software and Information Engg., Cairo, Egypt, 12-14, Nov. 2021, pp. 41–46, 2022.

[29] W. Mao, Y. Lu, J. Liu, B. Ai, Z. Zhong, and Z. Ding, “Beamforming Design in Cell-Free Massive MIMO Integrated Sensing and Communication Systems,” *IEEE GLOBECOM 2023*, 4-8 Dec. 2023, Kuala Lumpur, Malaysia, pp. 546–551, IEEE Xplore, 2023.

[30] M. Abdelfatah, A. Zekry, and S. Elsayed, “Orthogonal Beamforming Technique for Massive MIMO Systems,” *Annals of Telecommunications, Springer Link*, pp. 1–19, Feb. 2024.

[31] R. Garg, P. Bhartia, I. J. Bahl and A. Ittipiboon, *Microstrip Antenna Design Handbook*, Artech House, MA, USA, 2001.

[32] I. J. Bahl and P. Bhartia, *Microstrip Antennas*, Artech House, Dedham, USA 1980.

[33] S.Haykin, *Adaptive Filter Theory*, 4th Ed, Pearson Education, 2002.

[34] M. Mishra and J. S. Roy, “Investigations on the Effect of Mutual Coupling in Smart Antenna using Adaptive Signal Processing Algorithm”, *IEEE International Conference on Applied Electromagnetics, Signal Processing and Communication (AESPC)*, Oct. 22-24, 2018, IEEE Xplore, 1–5, 2018.